INSTITUTE OF PHYSICS PUBLISHING NANOTECHNOLOGY
Nanotechnology **15** (2004) 1524–1529 PII: S0957-4484(04)83271-9

Polyaniline nanowire synthesis templated by DNA

Patrick Nickels, Wendy U Dittmer, Stefan Beyer, Jörg P Kotthaus and Friedrich C Simmel

Department of Physics and Center for Nanoscience, LMU München
Geschwister-Scholl-Platz 1, 80539 Munich, Germany

Received 7 July 2004, in final form 23 August 2004
Published 10 September 2004
Online at stacks.iop.org/Nano/15/1524
doi:10.1088/0957-4484/15/11/026

Abstract
DNA-templated polyaniline nanowires and networks are synthesized using three different methods. The resulting DNA/polyaniline hybrids are fully characterized using atomic force microscopy, UV–vis spectroscopy and current–voltage measurements. Oxidative polymerization of polyaniline at moderate pH values is accomplished using ammonium persulfate as an oxidant, or alternatively in an enzymatic oxidation by hydrogen peroxide using horseradish peroxidase, or by photo-oxidation using a ruthenium complex as photo-oxidant. Atomic force microscopy shows that all three methods lead to the preferential growth of polyaniline along DNA templates. With ammonium persulfate, polyaniline can be grown on DNA templates already immobilized on a surface. Current–voltage measurements are successfully conducted on DNA/polyaniline networks synthesized by the enzymatic method and the photo-oxidation method. The conductance is found to be consistent with values measured for undoped polyaniline films.

(Some figures in this article are in colour only in the electronic version)

1. Introduction

The highly specific molecular recognition processes between DNA strands with complementary base sequences form the basis of DNA self-assembly. In contrast to other self-assembly strategies, DNA-based approaches offer the significant advantage of sequence programmability and therefore the potential to construct nontrivial assemblies [1, 2]. Whereas conventional self-assembly processes such as the formation of self-assembled monolayers lead to structures with very low information content (periodic assemblies), DNA, in principle, can be used to produce non-periodic and complex structures. A large variety of such DNA-based nanoconstructs have been demonstrated in recent years: for example, geometric objects like cubes [3] and octahedra [4], or various two-dimensional assemblies [5–7]. The power of DNA-based algorithmic self-assembly has recently been shown by the construction of a Sierpinski triangle [8]. Utilizing its mechanical properties, DNA can even be used to build dynamic nanoscale actuators (see e.g., [9–11]).

One of the most challenging goals of molecular nanotechnology is the self-assembly of a molecular computer. Whereas great progress has been made in the electronic characterization of single molecules, there are only few convincing concepts for the assembly of electronic circuits made from molecules [12]. It is therefore of great interest to explore whether the unique self-assembly properties of DNA can be exploited for the construction of nanoscale electronic circuits. Recent detailed investigations into the conductivity of DNA molecules have shown that DNA is an extremely poor conductor [13–18]. To build electronic circuits with the help of DNA therefore requires attachment of electronically functional materials to DNA [13, 19–31] or an appropriate chemical modification of DNA itself [32–34]. At the same time, the molecular recognition properties of DNA should not be compromised by these modifications. DNA has already been shown to be a template for the directed growth of metals [13, 19–23], semiconductor nanoparticles [24, 25] and conductive polymers [26–30]. Successful electronic transport measurements have predominantly been performed with DNA-templated metal wires so far—with the exception of the ingenious DNA-directed assembly of a carbon nanotube based field effect transistor [31]. Metal wires are only useful as interconnects for electronically functional structures like

diodes or transistors. It is therefore of great importance to the field of DNA-based electronics to find materials with interesting electronic properties which are compatible with DNA technology. Obvious candidates are conductive polymers such as polypyrrole, polyaniline (PAni) [27–30] or poly(phenylenevinylene) (PPV) [26] which are based on cationic monomers or precursors and can therefore potentially be synthesized along the negatively charged sugar–phosphate backbone of DNA. We here present a full comparative study of three different methods for the synthesis of the conductive polymer polyaniline templated on DNA, including *I–V* measurements. Synthesis is performed both in solution and on a surface. The resulting DNA/PAni complexes are stretched on different substrates (mica and silicon) and characterized using atomic force microscopy (AFM). UV–vis spectroscopy gives spectroscopic evidence for the formation of polyaniline. DC transport measurements performed on undoped DNA/PAni wires yield conductance values consistent with those obtained for weakly conducting polyaniline films.

2. Experimental details

2.1. Template-directed synthesis of polyaniline

Polyaniline is a conductive polymer which can be synthesized by oxidative polymerization from its monomer aniline. At low pH values aniline ($pK_b = 9.4$) is protonated to form the positively charged anilinium ion, and it can be exchanged as a counterion for the negatively charged sugar–phosphate backbone of DNA. Here, three different methods were employed to synthesize polyaniline on DNA. A mild oxidative method using horseradish peroxidase (HRP) and hydrogen peroxide, a photo-oxidation method using ruthenium tris(bipyridinium) ($Ru(bpy)_3^{2+}$) complexes, and a harsh method using ammonium persulfate (APS) as an oxidation agent. The latter method was also used to polymerize polyaniline along DNA strands immobilized to a substrate. λ-DNA (New England Biolabs) with a length of 16.5 μm (48.5 kbp) was used as the DNA template in all cases. Before modification, the DNA was purified by precipitation in isopropanol. If not stated otherwise, all chemicals were purchased from Sigma-Aldrich and used without further purification. In all cases, polyaniline was synthesized at moderately low pH values of 3–5 to prevent DNA damage.

2.1.1. Horseradish peroxidase/hydrogen peroxide method. This method is adapted from [27]. The biological oxidoreductase horseradish peroxidase (HRP) catalyses the reduction of hydrogen peroxide which is accompanied by the oxidation of another molecule. In the presence of both aniline and hydrogen peroxide, HRP catalyses the oxidative polymerization of polyaniline under relatively mild reaction conditions. To facilitate polyaniline synthesis along DNA templates, λ-DNA (25 μg ml^{-1}) was typically incubated for 20–60 min in 100 μl aniline solution (1.92 mM in phosphate buffer, pH = 4.3). This corresponds to a ratio of aniline to DNA phosphate groups of 25:1. To this solution 5 μl HRP (5 mg ml^{-1}) was added, followed by the addition of 16 μl H_2O_2 (0.03% in H_2O). Hydrogen peroxide was added in four aliquots of 4 μl. After 90 min of reaction, the resulting polyaniline/DNA wires were characterized using UV–vis spectroscopy or stretched on a substrate for AFM imaging and electrical characterization as described below.

2.1.2. Ruthenium tris(bipyridinium) method. This method is adapted from [28, 29]. The ruthenium tris(bipyridinium) ($Ru(bpy)_3^{2+}$) complex strongly absorbs light of wavelengths around 450 nm. In the photo-excited state it can oxidize other species by oxidative electron transfer. For polyaniline synthesis, DNA was added to a solution of *N*-phenylene phenyldiamine (1 mM in H_2O, adjusted to pH = 3 with HCl) to yield a final concentration of 25 μg ml^{-1} and a total volume of 120 μl. To this solution, 1 μl of the ruthenium complex (1 mM in H_2O) was pipetted, followed by mixing. The photo-oxidation was initiated by illuminating the reaction vial with a mercury lamp ($P = 100$ W) through a band pass filter ($\lambda = 470$–490 nm). The reaction was typically maintained for 60 min.

2.1.3. Ammonium persulfate method. For synthesis of polyaniline on DNA templates immobilized on a chip surface, the chip was first incubated for 20–60 min in a 1–100 mM aniline solution in phosphate buffer (pH = 4.3). After thoroughly rinsing the chip with deionized water, it was incubated in a 1 mM solution of $(NH_4)_2S_2O_8$ for 20 min to polymerize the aniline monomers bound to the DNA. The reaction was stopped by extensive rinsing with deionized water and drying of the chip under a flow of nitrogen gas. This procedure could be applied repeatedly to the chips which resulted in denser coating of the DNA with polyaniline.

Ammonium persulfate was also used to synthesize polyaniline templated by DNA in solution. Typically, to 50 μl of DNA (50 μg ml^{-1} in 10 mM phosphate buffer, pH = 4.3) 50 μl of a 77 μM solution of aniline was pipetted. After 20–60 min, 25 μl of ammonium persulfate solution (185 μM) was added to the reaction mixture. In this procedure, the ratio between phosphates, aniline and $(NH_4)_2S_2O_8$ was 2:1:1.2. When aniline was present in excess, this procedure led to the formation of large amounts of PAni not attached to DNA. On the other hand, at roughly equimolar ratio between aniline and phosphates only incomplete coverage of DNA by polyaniline could be achieved (see the discussion).

2.2. Spectroscopy

UV–vis spectroscopy was used to validate the synthesis of polyaniline wires and to monitor the reaction progress. Polyaniline has strong absorption bands around $\lambda = 350$–450 nm and between $\lambda = 750$–850 nm [35] whereas DNA has its typical strong absorption peak at $\lambda = 260$ nm. For longer π-conjugation lengths, the second peak in the polyaniline absorption spectrum can shift towards longer wavelengths [28]. Spectroscopic measurements were performed on a Jasco UV–vis spectrophotometer V-550.

2.3. DNA immobilization and AFM imaging

Before AFM characterization or for polyaniline synthesis on surface bound templates the DNA wires were immobilized on a solid substrate using molecular combing techniques [36, 37].

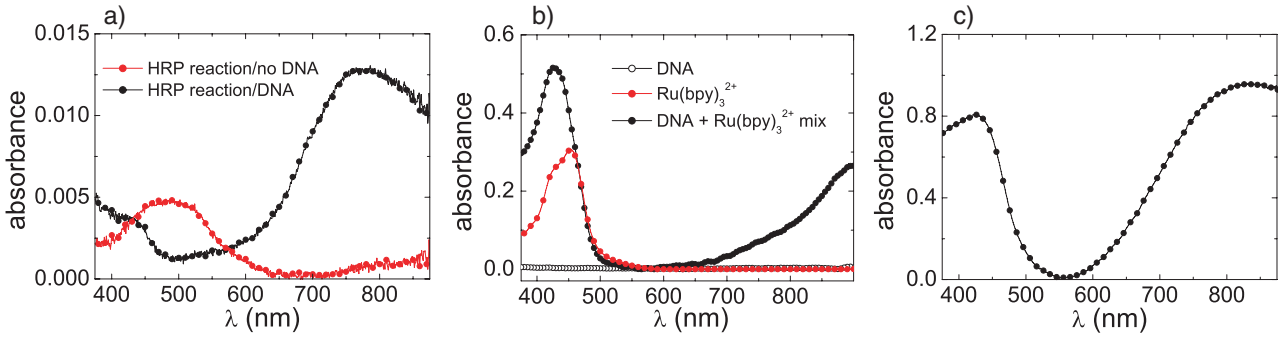

Figure 1. UV–vis spectra of polyaniline synthesized on DNA templates using three different methods. (a) HRP/H_2O_2 method: there is almost no polyaniline formation in the absence of DNA (red/grey curve). The peak at 500 nm is possibly due to the spurious formation of oligomers. In the presence of DNA, polyaniline is synthesized along the template as can be seen by the peaks at 400 and 800 nm. (b) $Ru(bpy)_3^{2+}$ method: the absorbance of the ruthenium complex (red/grey curve) overlaps with the low-wavelength absorbance band of PAni. However, the absorption at higher wavelengths shows formation of the polymer (black curve). (c) Absorbance of PAni synthesized with ammonium persulfate as oxidant.

For AFM characterization, the preferred substrate was mica. To the mica surfaces a 10 μl drop of a 2 mM aqueous solution of $MgCl_2$ was added, followed by 10 μl DNA solution (25–250 μg ml^{-1}) and another 10 μl drop of water. After each application of a solution the mica sample was spun on a spin coater for 90 s at 3000 rpm. A final spin for 90 s served to dry the sample. For electrical characterization, the wires were stretched between Au electrodes on a silicon substrate. To facilitate combing on silicon, the chips were treated with trimethylchlorosilane for two minutes and subsequently washed with hexane. A drop of DNA solution (1 μl) at a concentration of 50–250 μg ml^{-1} in MES buffer (2.4 mM, pH = 5.5) was deposited on the chip, left for one minute and then removed using filter paper. The receding meniscus of the droplet stretches and aligns the DNA molecules on the surface. AFM characterization of the immobilized DNA/Pani hybrids was performed in tapping mode with a Digital Instruments scanning probe microscope (Dimension 3100) with Nanoscope IIIa controller hardware.

2.4. Lithography and electronic measurements

Electrode structures were fabricated on n^+-doped silicon wafers with a 150 nm thick insulating oxide layer (Crystec GmbH, Germany) using standard optical and electron beam lithographic techniques. The optically defined electrodes had a thickness of 75 nm with a 5 nm adhesion layer of nickel–chromium or titanium. The electron beam written structures were 35 nm thick with a 5 nm adhesion layer. The electrical transport properties of the polyaniline/DNA hybrids connected to the electrodes were determined in a dry, temperature-controlled environment on a SUSS PM5 analytical probe system (Suss Microtec, Garching, Germany) in a standard two-point arrangement using a low-noise current amplifier (Femto DLPCA-200) close to the sample.

3. Results and discussion

3.1. Synthesis

UV–vis spectra recorded from the reaction solutions show that all three procedures described above successfully led to the synthesis of polyaniline (figure 1). The resulting spectra for the HRP/H_2O_2 method are shown in figure 1(a). Without DNA, almost no polyaniline is synthesized. In the presence of DNA, however, a clear absorption signal from polyaniline is observed. No absorption is detected from polyaniline when HRP is not added to the reaction. An absorption spectrum obtained from PAni synthesized by the $Ru(bpy)_3^{2+}$ method is shown in figure 1(b). The PAni absorption peak at ≈400 nm overlaps with the strong absorption of the ruthenium complex at ≈450 nm. However, the formation of polyaniline can be judged from the appearance of an absorption band at higher wavelengths. This absorption band is shifted towards 900 nm, which indicates that longer PAni chains are formed than in the other reactions. In figure 1(c), the absorbance of polyaniline synthesized using ammonium persulfate at pH = 4.3 is shown. The low aniline concentrations needed to observe preferential growth along DNA (see the next section) were too low to lead to measurable PAni absorbance values. The absorbance curves in figures 1(b) and (c) were therefore recorded from reaction solutions with higher aniline/oxidant concentrations. Under these conditions, DNA does not act as a template any more, and PAni synthesis takes place uniformly in solution. In contrast to the HRP method, DNA is not required for the formation of PAni using APS. However, due to the higher local concentration of anilinium ions along the sugar–phosphate backbone, DNA still acts as a template at very low reactant concentrations. Accordingly, for AFM imaging and I–V measurements, the concentrations were chosen much lower (see also the experimental sections). In order to be able to judge whether under low concentration conditions PAni synthesis preferentially took place along DNA templates, DNA/PAni samples were immobilized on surfaces and extensively investigated using atomic force microscopy.

3.2. AFM characterization

AFM images of DNA/PAni hybrids show the formation of polyaniline preferentially along DNA strands for all synthesis procedures adopted. In solution, the ammonium persulfate method could only be applied at low aniline concentrations. Otherwise a large amount of PAni not templated by DNA would be formed. However, working at low aniline concentrations

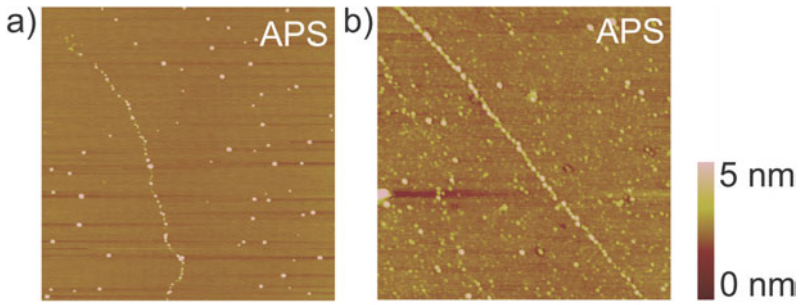

Figure 2. Topographic AFM images of polyaniline synthesized on DNA templates. (a) Synthesis was performed in solution, followed by stretching on mica (the image size is 4 μm $\times$ 4 μm). (b) DNA templates were first combed on a silanized silicon surface, followed by polyaniline synthesis on the substrate (the image size is 2 μm $\times$ 2 μm).

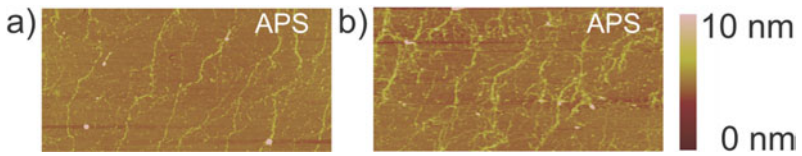

Figure 3. AFM images of polyaniline synthesized on DNA networks: (a) after one reaction cycle, (b) after a second application of the reaction solution to the network shown in (a). The size of the images is 5 μm $\times$ 2.5 μm in both cases.

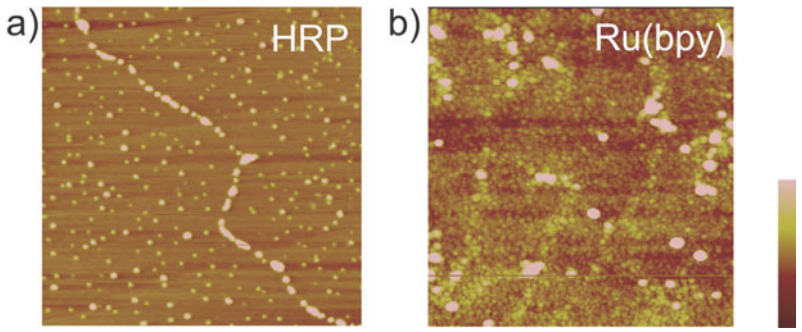

Figure 4. (a) AFM image of DNA/PAni synthesized by the HRP/H_2O_2 method in solution and stretched on a mica substrate. The image size is 2 μm $\times$ 2 μm; the height scale bar ranges from 0 to 5 nm. (b) DNA/PAni network synthesized by the $Ru(bpy)_3^{2+}$ method and stretched on a silicon substrate. The image size is 1.3 μm $\times$ 1.3 μm; the height scale bar ranges from 0 to 10 nm.

led to the formation of only isolated PAni particles along DNA (figure 2(a)). PAni/DNA hybrids could be well distinguished from pure DNA from height measurements. On topographic AFM images, DNA typically appears to be 0.5 nm in height. In contrast, PAni particles and wires were typically 5 nm in height or higher (see figures). One of the advantages of the persulfate method was the possibility to synthesize PAni on pre-immobilized DNA. An example of a chain of PAni particles synthesized along a DNA strand immobilized on a silanized silicon surface is shown in figure 2(b). The figure shows the formation of closely spaced particles of uniform size along the template. There is also some background deposition of PAni. To enhance the coverage of DNA with Pani, the reaction mixture could be applied to immobilized templates several times. This is exemplified in figure 3 with a DNA network which has been imaged after one and two synthesis cycles. Synthesis on a surface is not as effective with the other methods. The HRP/H_2O_2 method is compromised by protein adsorption on the surface. The $Ru(bpy)_3^{2+}$-based method could not be applied as the reaction mixture has to be strongly illuminated to support the photo-oxidation reaction. In solution, however, these methods also successfully led to the formation of DNA/PAni hybrids. AFM images of DNA/PAni wires synthesized by these methods are shown in figure 4. For the HRP/H_2O_2 method, PAni domains with a typical height of 5 nm formed uniformly along DNA (figure 4(a)) with some background formation of PAni remote from the template. DNA also acted as a template for the formation of PAni using the $Ru(bpy)_3^{2+}$ method; however, the resulting structures were much less uniform in height and tended to agglomerate (figure 4(b)). Stretching DNA/PAni hybrid structures between electrodes turned out to be more difficult than on a bare substrate. The molecular combing technique could not be applied effectively as the receding meniscus of the sample droplet preferentially moved parallel to the electrode gaps and therefore exerted a shearing force to the DNA strands. AFM imaging was difficult due to the large height difference between gold electrodes (40–80 nm) and the DNA/PAni hybrids. Furthermore, AFM images of samples prepared by the HRP/H_2O_2 method suffered from contamination by protein adsorption. Two examples of DNA/PAni networks spanning a 2 μm wide gap between electrodes are shown in figure 5. Whereas the HRP/H_2O_2 sample is highly contaminated, single DNA/PAni wires can be discerned on the AFM image of the

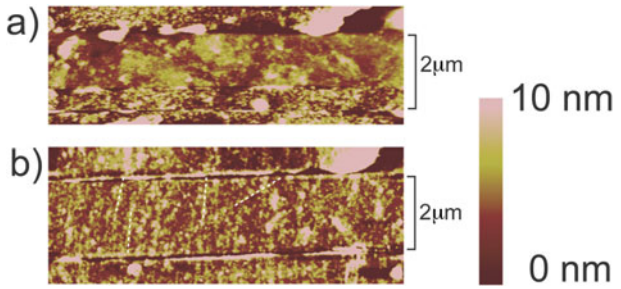

Figure 5. AFM images of polyaniline/DNA networks stretched between two electrodes. (a) Networks synthesized by the HRP/H_2O_2 method, (b) synthesized by the $Ru(bpy)_3^{2+}$ method. The electrode spacing of 2 μm is indicated. The lines in (b) are drawn as a guide for the eye. The height scale is 0–20 nm.

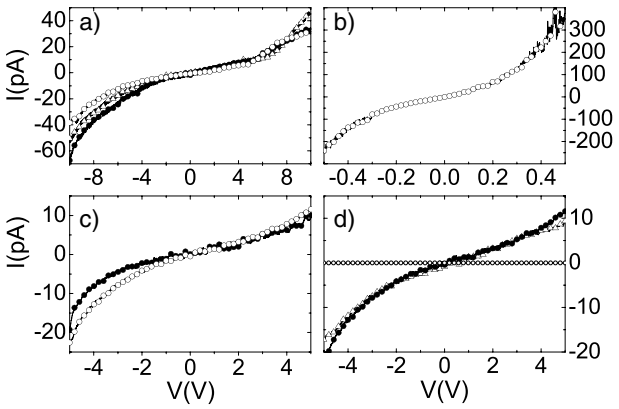

Figure 6. (a) I–V curves measured with three different samples of DNA/PAni networks synthesized by the HRP/H_2O_2 method placed between electrodes with a 2 μm spacing (as in figure 5(a)); (b) as in (a), measured with electrodes with a 200 nm spacing; (c) I–V curves measured on two DNA/Pani samples synthesized by the $Ru(bpy)_3^{2+}$ method (cf figure 5(b)); (d) comparison of I–V-curves synthesized by the two methods (triangles: HRP/H_2O_2 method; closed circles: $Ru(bpy)_3^{2+}$ method) and control measurement for unmodified DNA (open circles).

$Ru(bpy)_3^{2+}$ sample. In the case of the HRP/H_2O_2 sample, the excessive protein adsorption is probably mediated by the silanization [38].

3.3. Electronic properties

The electronic properties of the DNA/PAni networks were investigated using samples as shown in figure 5. The samples were extensively washed in deionized water and dried thoroughly after the application of the DNA networks to avoid conduction by water and salt films. All experiments were carried out at room temperature. Control experiments on unmodified DNA performed before PAni synthesis yielded sample resistances >10 TΩ without exception ($I < 1$ pA at $V = 10$ V applied voltage; see figure 6(d)). We were also unable to drive a current through networks prepared by the ammonium persulfate method, even after the application of several reaction cycles to the sample as described in the previous section. Control experiments performed on continuous polyaniline films prepared by the same method with larger amounts of reagents led to the expected conductivity values. We therefore conclude that the APS method in principle could produce polyaniline; however, the coverage of the DNA templates was not dense enough to allow for a current to flow through the network. It is also conceivable that the DNA templates are degraded by the strong oxidation agent, leading to discontinuities in the PAni wires. Typical I–V curves obtained with samples prepared by the other methods are shown in figure 6. All curves show similar, slightly rectifying behaviour with conductances in the range of 2–5 pS (2 μm electrode spacing) and 0.1–1 nS (200 nm electrode spacing) as expected for a weakly semiconducting material. As displayed in figure 6(d), samples prepared by the HRP/H_2O_2 method and the $Ru(bpy)_3^{2+}$ method show nearly identical behaviour in the voltage range between -5 and 5 V. To rule out conduction by other components than the DNA/PAni networks, additional control experiments were performed on HRP films and on $Ru(bpy)_3^{2+}$ solutions applied to the surface. These experiments did not lead to measurable currents. A finite current was only measured when all the components necessary to synthesize polyaniline on DNA were present. It cannot be ruled out, however, that spurious PAni not formed on the DNA templates also contributes to conduction. To compare the results of our measurements with literature values for the conductivity of polyaniline, we can make a simple estimate: if we assume that of the order of $\sim$100 wires with $\sim$5 nm diameter connect the two electrodes, a conductance of 1 pS corresponds to a conductivity of $\approx 1 \times 10^{-5}$ S cm^{-1}. The measured conductance values therefore are consistent with values expected for undoped polyaniline base [39]. It is clear, however, that the values measured are not determined by the conduction properties of bulk polyaniline. Current flow will also be strongly affected by discontinuities between conducting domains (see figure 4) and by contact resistances between the networks and the electrodes. This is also expressed in the higher conductance obtained in the measurement with the more closely spaced electrodes (figure 6(b)). Even though the electrodes are only tenfold closer, the conductance increases by a factor of 100. This is probably due to the considerably higher probability of finding a conducting path through the network connecting the electrodes. To further elucidate the conduction mechanisms leading to the currents measured in the experiments described above, additional experiments are required. In particular, the influence of temperature and doping level on the conduction has to be determined. Preliminary attempts to dope the wires using hydrochloric acid did not lead to improved conductance values. It is assumed that subsequent washing with deionized water could 'undope' the wires again [40]. One also has to investigate the influence of the contact resistance between the DNA/PAni networks and the electrodes. To improve the contact resistance, it would be important to have a technique to deposit electrodes after the deposition of the networks on the substrate without damaging the PAni. We already performed some preliminary experiments on electroless deposition of gold on top of lithographically defined electrodes coated with DNA/PAni networks following a procedure described by Seidel *et al* [41]. So far, this did not lead to improved conductivity. Another possibility would be to make contact to the samples using electrodes on elastomeric stamps, a technique which has already successfully been used to contact other organic materials [42].

4. Conclusion

We have shown that polyaniline can be synthesized on DNA templates by three different methods. DNA templating seems to work best for polyaniline formed by oxidative polymerization of aniline with ammonium persulfate, both in solution and on templates immobilized on a chip. DNA also is a good template for polyaniline formed by enzymatically catalysed polymerization utilizing horseradish peroxidase. However, immobilization of these structures between contact electrodes is compromised by extensive protein adsorption to the surface. A photo-oxidation method using ruthenium tris(bipyridinium) complexes as photo-oxidant results in less uniform DNA/PAni structures than the other methods. On the other hand, electronic characterization of the resulting DNA/PAni hybrids was only successful for the enzymatic synthesis protocol and the photo-oxidation method. For the DNA/PAni networks investigated, the measured conductance values are consistent with those expected for undoped polyaniline. Additional experiments have to be conducted to improve the conduction properties of the DNA/PAni wires and to possibly utilize the promising protocol for the synthesis of polyaniline on surface-bound DNA templates.

Acknowledgments

This work is supported through the Emmy Noether program of the Deutsche Forschungsgemeinschaft (DFG). WUD acknowledges support by the Alexander von Humboldt foundation.

References

[1] Seeman N C *et al* 1998 *Nanotechnology* **9** 257–73
[2] Seeman N C 2003 *Nature* **421** 427–31
[3] Chen J H and Seeman N C 1991 *Nature* **350** 631–3
[4] Zhang Y W and Seeman N C 1994 *J. Am. Chem. Soc.* **116** 1661–9
[5] Winfree E, Liu F R, Wenzler L A and Seeman N C 1998 *Nature* **394** 539–44
[6] Mao C D, Sun W Q and Seeman N C 1999 *J. Am. Chem. Soc.* **121** 5437–43
[7] Yan H, Park S H, Finkelstein G, Reif J H and LaBean T H 2003 *Science* **301** 1882–4
[8] Rothemund P W K, Papadakis N and Winfree E 2004 submitted
[9] Mao C D, Sun W Q, Shen Z Y and Seeman N C 1999 *Nature* **397** 144–6
[10] Yurke B, Turberfield A J, Mills A P, Simmel F C and Neumann J L 2000 *Nature* **406** 605–8
[11] Feng L P, Park S H, Reif J H and Yan H 2003 *Angew. Chem. Int. Edn Engl.* **42** 4342–6
[12] Heath J R, Kuekes P J, Snider G S and Williams R S 1998 *Science* **280** 1716–21
[13] Braun E, Eichen Y, Sivan U and Ben-Yoseph G 1998 *Nature* **391** 775–8
[14] Porath D, Bezryadin A, de Vries S and Dekker C 2000 *Nature* **403** 635–8
[15] de Pablo P J, Moreno-Herrero F, Colchero J, Herrero J G, Herrero P, Baro A M, Ordejon P, Soler J M and Artacho E 2000 *Phys. Rev. Lett.* **85** 4992–5
[16] Cai L T, Tabata H and Kawai T 2000 *Appl. Phys. Lett.* **77** 3105–6
[17] Storm A J, van Noort J, de Vries S and Dekker C 2001 *Appl. Phys. Lett.* **79** 3881–3
[18] Cai L T, Tabata H and Kawai T 2001 *Nanotechnology* **12** 211–6
[19] Richter J, Seidel R, Kirsch R, Mertig M, Pompe W, Plaschke J and Schackert H K 2000 *Adv. Mater.* **12** 507
[20] Richter J, Mertig M, Pompe W, Monch I and Schackert H K 2001 *Appl. Phys. Lett.* **78** 536–8
[21] Richter J, Mertig M, Pompe W and Vinzelberg H 2002 *Appl. Phys.* A **74** 725–8
[22] Keren K, Krueger M, Gilad R, Ben-Yoseph G, Sivan U and Braun E 2002 *Science* **297** 72–5
[23] Richter J 2003 *Physica* E **16** 157–73
[24] Coffer J L, Bigham S R, Li X, Pinizzotto R F, Rho Y G, Pirtle R M and Pirtle I L 1996 *Appl. Phys. Lett.* **69** 3851–3
[25] Dittmer W U and Simmel F C 2004 *Appl. Phys. Lett.* **85** 633–5
[26] Eichen Y, Braun E, Sivan U and Ben-Yoseph G 1998 *Acta Polym.* **49** 663–70
[27] Nagarajan R, Liu W, Kumar J, Tripathy S K, Bruno F F and Samuelson L A 2001 *Macromolecules* **34** 3921–7
[28] Uemura S, Shimakawa T, Kusabuka K, Nakahira T and Kobayashi N 2001 *J. Mater. Chem.* **11** 267–8
[29] Kobayashi N, Uemura S, Kusabuka K, Nakahira T and Takahashi H 2001 *J. Mater. Chem.* **11** 1766–8
[30] Ma Y F, Zhang J M, Zhang G J and He H X 2004 *J. Am. Chem. Soc.* **126** 7097–101
[31] Keren K, Berman R S, Buchstab E, Sivan U and Braun E 2003 *Science* **302** 1380–2
[32] Maeda Y, Tabata H and Kawai T 2001 *Appl. Phys. Lett.* **79** 1181–3
[33] Lee H Y, Tanaka H, Otsuka Y, Yoo K H, Lee J O and Kawai T 2002 *Appl. Phys. Lett.* **80** 1670–2
[34] Gu J H, Tanaka S, Otsuka Y, Tabata H and Kawai T 2002 *Appl. Phys. Lett.* **80** 688–90
[35] Stafstrom S, Bredas J L, Epstein A J, Woo H S, Tanner D B, Huang W S and MacDiarmid A G 1987 *Phys. Rev. Lett.* **59** 1464–7
[36] Bensimon A, Simon A, Chiffaudel A, Croquette V, Heslot F and Bensimon D 1994 *Science* **265** 2096–8
[37] Bensimon D, Simon A J, Croquette V and Bensimon A 1995 *Phys. Rev. Lett.* **74** 4754–7
[38] Sigal G B, Mrksich M and Whitesides G M 1998 *J. Am. Chem. Soc.* **120** 3464–73
[39] Stejskal J, Hlavata D, Holler P, Trchova M, Prokes J and Sapurina I 2004 *Polym. Int.* **53** 294–300
[40] Menon R, Yoon C O, Moses D and Heeger A J 1998 *Handbook of Conducting Polymers* ed T A Skotheim, R L Elsenbaumer and J R Reynolds (New York: Dekker)
[41] Seidel R, Liebau M, Duesberg G S, Kreupl F, Unger E, Graham A P, Hoenlein W and Pompe W 2003 *Nano Lett.* **3** 965–8
[42] Zaumseil J, Someya T, Bao Z N, Loo Y L, Cirelli R and Rogers J A 2003 *Appl. Phys. Lett.* **82** 793–5